Electrical Engineering in Japan, Vol. 142, No. 1, 2003
Translated from Denki Gakkai Ronbunshi, Vol. 121-D, No. 11, November 2001, pp. 1155–1162

A Sensorless Drive System for Brushless DC Motors Using a Digital Phase-Locked Loop

YOKO AMANO (formerly BING HONG XU),[1] TOSHIO TSUJI,[2] ATSUSHI TAKAHASHI,[3] SHIGEO OUCHI,[3] KYOJI HAMATSU,[1] and MASAHIKO IIJIMA[1]
[1]Yamamoto Electric Corporation, Japan
[2]Hiroshima University, Japan
[3]Fukushima Technology Center, Japan

SUMMARY

This paper proposes a sensorless drive system for Brushless DC (BLDC) motors using a Digital Phase-Locked Loop (DPLL). The Back Electromotive Force (BEMF) voltage is measured from the motor winding to determine the permanent magnet rotor position using the DPLL, and Pulse Width Modulation (PWM) limits the motor current to control the speed of BLDC motors. The proposed method can drive BLDC motors using an open-loop control without stepping out. Also, the proposed method is compared experimentally with a control method that uses Hall sensors. Experimental results for the BLDC motor show the effectiveness of the proposed method. © 2002 Wiley Periodicals, Inc. Electr Eng Jpn, 142(1): 57–66, 2003; Published online in Wiley InterScience (www.interscience.wiley.com). DOI 10.1002/eej.10074

Key words: position sensorless driver; digital phase-locked loop; PWM current control; back electromotive force; brushless DC motor.

1. Introduction

Brushless DC (BLDC) motors have the features of smaller size, higher efficiency, and better controllability than induction motors. In recent years, research on reduction of motor costs and drive systems has been intensively conducted [1–4]. In order to perform current control and speed control according to the permanent magnet rotor position, various position sensors such as encoders, resolvers, and magnetic Hall sensors are necessary [5]. However, these position sensors are very expensive, and produce complex problems involving motor assemblers, and wiring between a sensor board and a drive circuit. Thus, many efforts to realize light weight, compact size, and low price of BLDC motors without position sensors have been reported [6–22].

Most of the proposed methods without position sensors can be broadly subdivided into two approaches. One approach is to estimate the initial rotor position without position sensors in the stopped state of the rotor [7–10]. The other approach is that, after the BLDC motor rotates, the BLDC motor speed is controlled without position sensors [11–22]. The latter approach is especially considered in this paper.

Yang and colleagues [11] proposed a position sensorless control that estimates the position and speed of BLDC motors in the running state. Their idea is to create an adaptation observer based on the model reference adaptive control. Tomita and colleagues [12] introduced an adaptive sliding observer for the sensorless speed control of BLDC motors. Moreover, Hanamoto and colleagues [13] presented a sensorless method of control of BLDC motors using an extended Back Electromotive Force (BEMF) observer. Also, Bolognani and colleagues [14] proposed a rotor position estimation algorithm with an extended Kalman filter. Tatematsu and colleagues [15] presented a sensorless driver that estimates the rotation speed by using a low-level linear observer. In addition, an algorithm for rotor position estimation using the current vector when power is supplied again has been reported [16]. Neuro-fuzzy compensation of rotor position estimation errors has been proposed [17]. Although all of the methods listed above use an open loop for starting the BLDC motor, the BLDC motor

Contract grant sponsor: Funded in part by an Intensive Development Research Promotion Enterprise Subsidy of the Fukushima Technology Center 1998.

may start with stepping out and the drive systems are very complicated.

On the other hand, investigations of sensorless drive using the BEMF of the BLDC motor have been pursued [18–22]. Although some approaches with an electrical drive angle of 120° have achieved practical use, they are limited to specific low to middle speed applications, such as cooling fan motors and hard disk motors [21]. Moreover, they are especially influenced by power voltage changes and high-frequency noise, and applications with high rotation speed are very difficult [18]. In particular, sensorless drive with an electrical drive angle of 180° is more complicated than that with an electrical drive angle of 120°, and few applications are currently in existence.

In this paper, a new sensorless drive system based on the approach of Ref. 19 using a Digital Phase-Locked Loop (DPLL) and the BEMF voltage is proposed. The proposed method can be applied to a wide rotation range, and can achieve a reduction of magnetic noise and an improvement in the efficiency of the BLDC motor. Moreover, in order to rotate the BLDC motor smoothly without stepping out at the motor stopping position, a new starting sequence of the BLDC motor is proposed. The drive system is very compact and low in cost. In this paper, the proposed method is experimentally compared with a control method using a Hall sensor [23]. Experimental results for the BLDC motor show the effectiveness of the proposed method.

2. The Sensorless Drive System

The composition of the sensorless drive system using Pulse Width Modulation (PWM) current control and a position detector without a position sensor is shown in Fig. 1. The drive system connects the BLDC motor with an inverter via the motor windings, and drives the BLDC motor using current control. For position detection without the position sensor, the BEMF is detected from the motor windings, and for PWM current control, the line current of

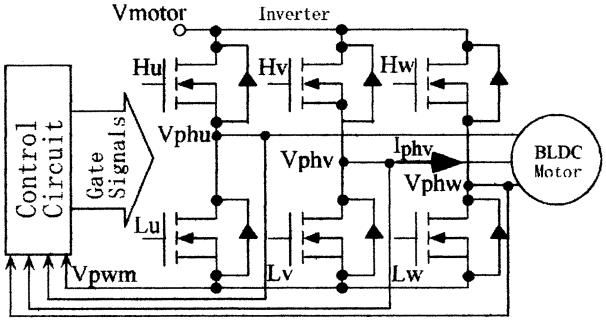

Fig. 1. Sensorless drive system.

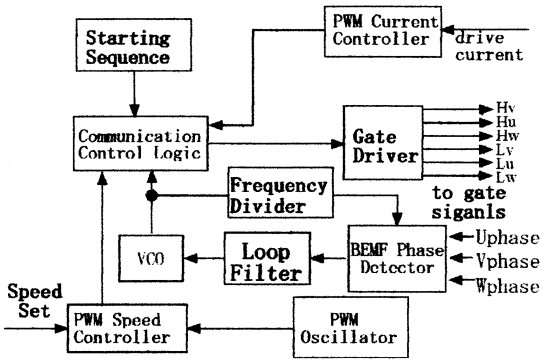

Fig. 2. Block diagram of the sensorless drive system.

the BLDC motor is measured from the source of Field Effect Transistor (FET) power devices in the inverter. Figure 2 shows a block diagram of the sensorless drive system. First, the communication control logic outputs gate drive signals to rotate the BLDC motor at a suitable speed appropriate to the dynamic characteristics of the BLDC motor. The DPLL consists of a Voltage-Controlled Oscillator (VCO), a loop filter, a BEMF phase detector, and a frequency divider. Second, the DPLL detects the rotor position without the position sensor, and outputs a frequent pulse appropriate to the BEMF's phase to the communication control logic. Based on the speed setting, a PWM speed controller outputs a modulated pulse to the communication control logic. Next, the communication control logic synthesizes the two input signals and outputs the gate drive signals to the inverter through a gate driver. Finally, speed control of the BLDC motor is realized.

3. Position Sensorless Detection

When the rotor position is detected from the BEMF voltage, rotational unevenness and voltage change may occur due to the resistance, inductance, and impedance of the BLDC motor. We need an approach that extracts only rotor position information [20]. In this paper, a new method of detecting the rotor position without the position sensor using the DPLL is proposed, and the basic composition of the DPLL is shown in Fig. 3. From Fig. 3, the loop filter reduces various kinds of noise, and the VCO outputs a frequency pulse following the control voltage signal (a direct current voltage) from the loop filter. Then a digital frequency divider divides the frequency pulse and removes analog noise and voltage drops from the motor windings.

Although the DPLL originally contains nonlinear elements, the DPLL's operation is analyzed by automatic control theory [24, 25] in many cases. We analyze the

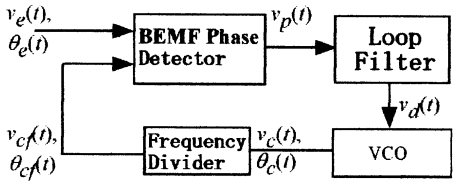

Fig. 3. Block diagram of the DPLL.

operation of the DPLL by Laplace conversion within the tolerance level of the drive system.

The BEMF phase detector shown in Fig. 3 generates a voltage signal $v_p(t)$ that corresponds to the phase angle difference between the BEMF signal $v_e(t)$ and the feedback signal $v_{cf}(t)$. The loop filter smoothes the signal $v_p(t)$ and outputs the control voltage signal $v_d(t)$ to the VCO, which changes the frequency of the frequency pulse by means of the control voltage signal. In Fig. 3, $\theta_e(t)$, $\theta_{cf}(t)$, and $\theta_c(t)$ are respectively the phases of the signals $v_e(t)$, $v_{cf}(t)$, and $v_c(t)$. Here, the BEMF is detected by comparing the motor winding's voltage with a standard voltage [21].

Because the loop filter removes inductive noise and high-frequency noise accompanying motor rotation and acquires a control voltage signal without ripple, the response characteristic of the DPLL open loop plays an important role. However, the DPLL is a negative feedback device, and if the output signal phase delay of the DPLL open loop is 180° at the same time as the gain of the DPLL open loop is 1, then the DPLL open loop will become unstable.

Let us analyze the operation of the loop filter shown in Fig. 4 and derive the design formula of each component element. The transfer function $F(s)$ of the loop filter is

$$F(s) = \frac{sRC_2 + 1}{s^2RC_1C_2 + s(C_1 + C_2)} \tag{1}$$

When the frequency divider of Fig. 3 is a programmable divider and its time delay is sufficiently small, the transfer function of the frequency divider can be defined as $1/N$.

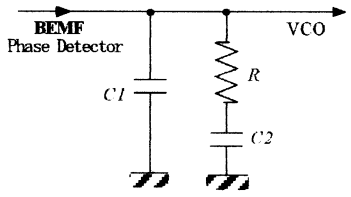

Fig. 4. Structure of the loop filter.

Also, the VCO performs integration of the control voltage signal, and the transfer function of the VCO can be denoted as K_v/s, where K_v is a gain [24]. Then, the transfer function $H_L(s)$ of the DPLL open loop is described by

$$H_L(s) = K_pF(s)\frac{K_v}{s}\frac{1}{N} \tag{2}$$

Since the BEMF phase detector makes an input signal that contains the BEMF signal $v_e(t)$ and the frequency divider's output $v_{cf}(t)$, and outputs a voltage signal $v_p(t)$ according to the phase difference of the input signal, the characteristic of the BEMF phase detector is approximately given as a gain K_p.

Substituting Eq. (1) into Eq. (2), the transfer function $H_L(s)$ becomes

$$H_L(s) = \frac{K_pK_v}{N}\frac{sRC_2 + 1}{s^2[sRC_1C_2 + (C_1 + C_2)]} \tag{3}$$

Since Eq. (3) has two poles at the origin of the complex plane, the phase delay of Eq. (3) shifts by 180°, and the DPLL open loop may become unstable. For stabilization of Eq. (3), where the amplitude $|H_L(j\omega)|$ is near 1, the transfer function $H_L(s)$ must perform leading phase compensation. This can assure a suitable phase margin near the gain crossover frequency, and the stability of the DPLL is improved. When the loop gain K_L is defined as $K_L = K_pK_v/N$, the transfer function $H_L(s)$ of Eq. (3) is rewritten as

$$H_L(s) = K_L\frac{s + \omega_z}{s^2C_1(s + \omega_p)} \tag{4}$$

where ω_p and ω_z are the angular frequencies of the pole and the zero, respectively,

$$\omega_p = (C_1 + C_2)/(RC_1C_2) \tag{5}$$

$$\omega_z = 1/(RC_2) \tag{6}$$

If the angular frequency ω_p is Λ times the angular frequency ω_z, the angular frequency ω_p is written as

$$\omega_p = \Lambda\omega_z \tag{7}$$

When maximum phase leading is used to cover the motor speed range, the maximum leading angle frequency ω_g is the geometric average of the angular frequencies ω_z and ω_p, and is described by

$$\omega_g = \sqrt{\omega_z\omega_p} = \sqrt{\Lambda}\omega_z \tag{8}$$

In order to raise the phase margin of the DPLL open loop, a loop filter is designed based on the maximum

leading angle frequency. For a unit step response of Eq. (4), the stable time t_s is given by

$$t_s = -\ln(\frac{\rho}{100})/\zeta\omega_n \tag{9}$$

where ζ is the attenuation coefficient, ω_n is the natural angular frequency, and ρ is a setting constant that indicates the stability of the DPLL open loop [25].

Within N_c cycles, the stable time t_s that stabilizes the response of the DPLL open loop is rewritten as

$$t_s = N_c/f_m \tag{10}$$

where f_m is the average frequency of the BLDC motor's speed. The angular frequency ω_g of the secondary loop filter of Eq. (4) is defined as

$$\omega_g = 2\zeta\omega_n \tag{11}$$

By means of Eqs. (9) and (10), Eq. (11) can be rewritten as

$$\omega_g = -2\ln(\frac{\rho}{100})\frac{f_m}{N_c} \tag{12}$$

From Eqs. (8) and (12), the angular frequency ω_z is described as

$$\omega_z = -2\ln(\frac{\rho}{100})\frac{f_m}{N_c\sqrt{\Lambda}} \tag{13}$$

When maximum phase leading is performed at the angular frequency ω_g, the amplitude $|H_L(j\omega_g)|$ of Eq. (3) is set as 1, and the following formula is obtained:

$$|H_L(j\omega_g)| = K_L\frac{\sqrt{\omega_g^2+\omega_z^2}}{\omega_g^2 C_1\sqrt{\omega_g^2+\omega_p^2}} = 1 \tag{14}$$

Substituting Eqs. (8), (12), and (13) into Eq. (14), one capacitance C_1 of the loop filter is given by

$$C_1 = \frac{K_L N_c^2}{4\sqrt{\Lambda}\ln(\rho/100)^2 f_m^2} \tag{15}$$

From Eqs. (5) to (7), capacitance C_2 is

$$C_2 = C_1(\Lambda - 1) \tag{16}$$

Also, by Eqs. (6), (13), and (16), the resistance of the loop filter is

$$R = 2\Lambda\ln(\rho/100)\frac{f_m}{N_c K_L(1-\Lambda)} \tag{17}$$

Thus, all elements of the loop filter can be designed.

4. Starting Sequence

Generally, the conventional starting techniques carry out a forced communication unrelated to the rotor position, and the BLDC motor may rotate with stepping out, or right-and-left vibration. It is difficult to choose a time from the rotor stop to the rotor rotation with a speed which can detect the BEMF signal; in most cases, the time is decided by trial and error. To rotate the BLDC motor without stepping out, the new starting sequence shown in Fig. 5 is proposed. This sequence consists of a position reset mode, a rotation acceleration mode, and a rotation speed control mode. Since the time length of each mode can be calculated with the equation of motion of the BLDC motor that takes account of the moments of inertia of the load and the rotor, and the loss from motor internal friction, by adjusting the reset time t_r and the acceleration time f_a, even if the load has a certain amount of change, the BLDC motor can be assured of rotation without stepping out.

Let us explain the starting sequence of Fig. 5. First, the rotor of the BLDC motor rotates from the present position to a predetermined reset position within the reset time t_r. Next, the rotor rotation accelerates to a fixed speed f_a within the acceleration time t_a. Then the BEMF phase detector can detect the BEMF signal, and the loop filter raises the direct-current voltage of the control voltage signal until the speed set voltage is reached. Finally, the rotation speed control mode is performed.

Within the reset time t_r, two FETs of the high side and one FET of the low side are turned on, and when the excitation current flows through the motor windings, the generated stator magnetic field locks the rotor at the predetermined reset position. However, if the time t_r is too long, the excitation current increases and the efficiency of the BLDC motor drops. Conversely, if the time t_r is too short, the rotor will be rotated without the predetermined reset position, and will return with stepping out. Therefore, the method of choosing the time t_r must be examined.

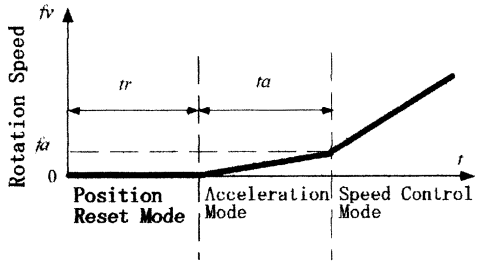

Fig. 5. Start-up sequence of BLDC motors.

By the dynamic characteristics of the BLDC motor, the relation between the rotation angle θ of the rotor and the reset torque τ for stopping the rotor at the predetermined reset position is represented as

$$\tau = J\frac{d^2\theta}{dt^2} \tag{18}$$

where J is the moment of inertia of the rotor and the load.

When the reset torque τ is proportional to the rotation angle θ between the present position and the predetermined reset position, the reset torque τ becomes

$$\tau = \kappa\theta \tag{19}$$

where θ is a sufficiently small angle [26], and κ is a reset torque constant related to the pole number and the torque constant of the BLDC motor [27].

Considering losses caused by such factors as eddy currents and motor internal friction, from Eqs. (18) and (19), we obtain the formula

$$J\frac{d^2\theta}{dt^2} + \sigma\frac{d\theta}{dt} - \kappa\theta = 0 \tag{20}$$

where σ is the loss constant. Solving Eq. (20), the resonance frequency f_r is obtained as

$$f_r = \sqrt{\frac{\kappa}{J}}/\gamma \tag{21}$$

where γ is the aggregate loss constant which contains various losses, such as nonlinear elements and the attenuation of the BLDC motor. Then, the reset time t_r can be written as

$$t_r = \gamma/\sqrt{\frac{\kappa}{J}} \tag{22}$$

In addition, the acceleration time t_a is proportional to the moment of inertia J and the gain K_v of the VCO, and is inversely proportional to the BEMF constant K_t of the BLEC motor, so that t_a is

$$t_a = \xi\frac{JK_v}{K_t} \tag{23}$$

where ξ is the acceleration constant.

5. Experimental Results

To illustrate the effectiveness of the proposed method, experiments using the proposed method and the control method using Hall sensors [23] were performed. The parameters of the experimental BLDC motor are shown in Table 1.

First, to minimize overshoot of the step response in the secondary loop filter, the setting time constant ρ and the attenuation coefficient ζ are set as 3 and 0.7 [28]. Since the DPLL must respond to the output signal of the VCO as quickly as possible and must realize stable speed control, when the cycle number of the DPLL is small, it is difficult to fully filter the output signal of the VCO within the short response time and to achieve stable speed control. However, if the cycle number of the DPLL is too large, the time locked at the predetermined reset position becomes long, and heat generation and energy loss of the BLDC motor occur until the rotor starts rotating. Also, the angular frequency ω_p and ω_z must cover the motor operating speed range, and if the angular frequency ω_p and ω_z are too far apart, electromagnetic noise readily enters the DPLL, and the rotational unevenness becomes large. We use the magnification $\Lambda = 10$ and the cycle number $N_c = 20$ chosen by trial and error. Because the average frequency f_m is proportional to the number of poles P of the BLDC motor and the geometric average value ω_g, $f_m = 0.2655 \cdot P \cdot \omega_p$ = 195 Hz and the loop gain $K_L = 0.02$ coul^2/kg-m^2 are calculated by Eq. (10). When the frequency f_{PWM} of the PWM is too low, audible noise caused by magnetic distortion arises, but if f_{PWM} is too high, the inverter switching loss is increased. Generally, f_{PWM} is set as 30 kHz.

In the proposed method, the electronic drive angle is 120°, and the frequency divider's N becomes 6. Since the total loss constant γ, the acceleration constant ξ, and the reset torque constant κ are related to complicated nonlinear factors, such as the tolerance of the power supply, the moment of inertia, and side friction, usually in a small motor the acceleration constant γ is chosen as 0.3 to 0.6, the acceleration constant ξ is within 0.5 to 0.9, and the reset torque constant κ is 0.4 to 0.8. A general method of determining these constants is a future subject of research. Here, γ = 4.28, ξ = 83.3, and κ = 0.7 Nm/A is calculated by the section 2-minute method [30]. The reset time t_r = 0.622 s

Table 1. Parameters of the BLDC motor used in the experiment

Items	Value
Pole number of motor	4
BEMF constant	0.0383 V·s/Rad
Inertia moment of rotor	1.85E-4 kg·cm^2
Inertia moment of load	25.15E-4 kg·cm^2
Winding resistance	0.136 Ω
Winding inductance	0.226 mH

and the acceleration time t_a = 0.108 s are computed from Eqs. (22) and (23).

Second, in the loop filter, C_1 = 1.291 μF, C_2 = 11.621 μF, and R = 3.997 kΩ are designed by Eqs. (15), (16), and (17). Figure 6 shows the Bode diagram of the DPLL open loop using the designed loop filter. When the amplitude is 0 dB, the phase compensation becomes about 55°; we can see that the DPLL open loop is stable.

When the inverter voltage is 12 V, the terminal voltage V_{phv} of the phase winding, the phase current I_{phv} (refer to Fig. 1), the output V_d of the loop filter, and the output V_c of the VCO (refer to Fig. 3) are as shown in Fig. 7. The loop filter smoothes the phase difference from the BEMF detector and outputs the control signal V_d to the VCO; in this way, the VCO outputs the frequency pulse to the communication control logic. These waveforms, like the good phase current, have arisen according to the phase relation of these signals. From Fig. 7 we can see that the position sensorless detection process is operating correctly.

Figure 8 shows experimental results in the steady state of the BLDC motor with a rotation speed of 10,158 rpm (1/Δ = 169.3 Hz). In Fig. 8 the gate signals V_v, V_u, and V_w are rectangular waveforms and are 120° apart from each other, and the phase current I_{phv} has a good waveform consistent with the gate signal. Thus, the BLDC motor is smoothly rotated at constant speed, and stable position sensorless control is realized.

The signals V_{pwm}, V_{lsu}, V_{lsw} and the phase current I_{phv} of Fig. 1 are shown in Fig. 9. The signal V_{pwm} is from the motor drive current using fixed off-time PWM current control, and gives the phase information of the PWM current control. We can see that one cycle of phase current I_{phv} corresponds to six pulses of the V_{pwm}, and the correct phase relation between the phase current and the gate signal is maintained at all times.

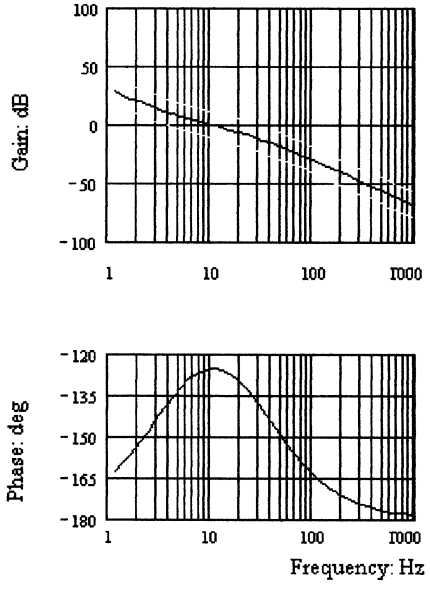

Fig. 6. Bode diagram of the open-loop transfer function of the DPLL.

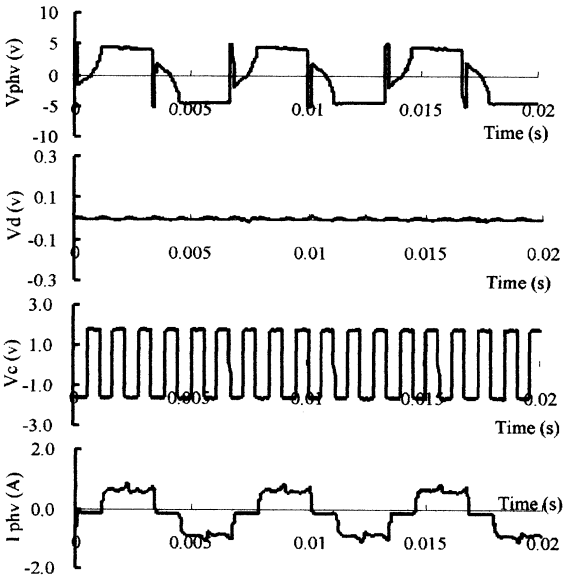

Fig. 7. Experimental results of sensorless control.

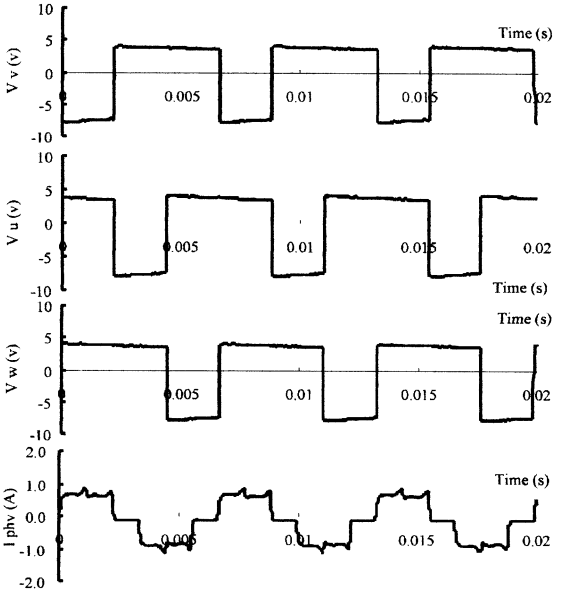

Fig. 8. Experimental results in steady state.

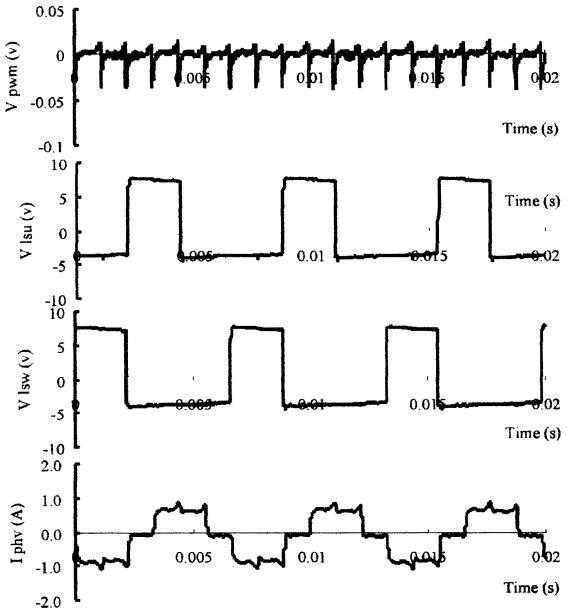

Fig. 9. Results of the PWM current control.

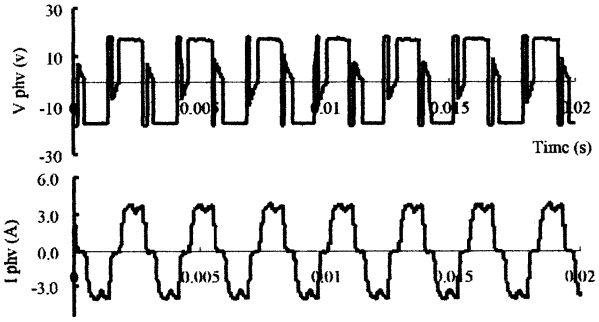

Fig. 11. Experimental results under high speed.

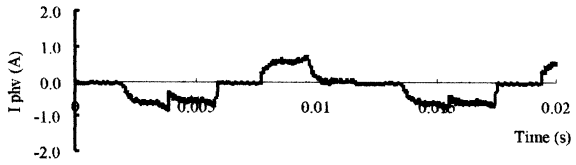

Fig. 12. Experimental results using speed control.

To check the speed control characteristic of the proposed method, an experiment was performed with a BLDC motor under changeable load. Figure 10 shows the phase current I'_{phv} without fan load and the phase current I_{phv} with fan load. The effective value of I'_{phv} is smaller than that of I_{phv}, but the periodic difference of the two waveforms is 0.6 Hz and their ratio is 0.6 Hz/85.84 Hz = 0.7014%. Even if the load of the BLDC motor changes from $1.85 \cdot 10^{-4}$kg·cm^2 to $2.7 \cdot 10^{-3}$kg·cm^2, or by a factor of about 15, the BLDC motor can rotate exactly at the set speed, and can always turn without stepping out.

To test the effectiveness of the proposed method at a high rotation speed, the inverter voltage was set as 35 V and the resistance and capacitance of the loop filter were de-

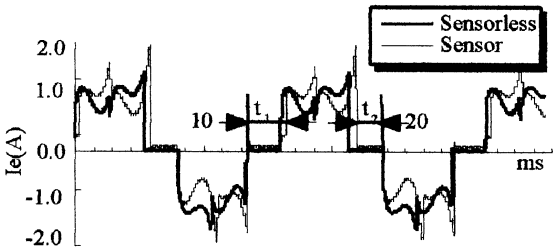

Fig. 13. Comparison of the experimental results.

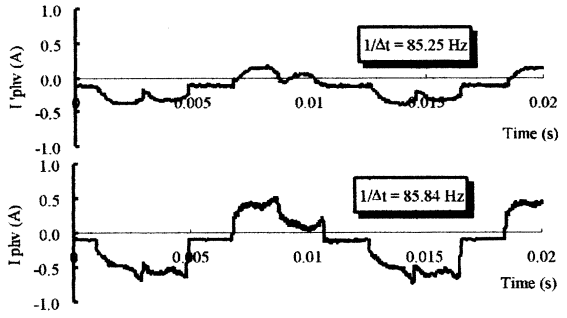

Fig. 10. Experimental results in the varied load.

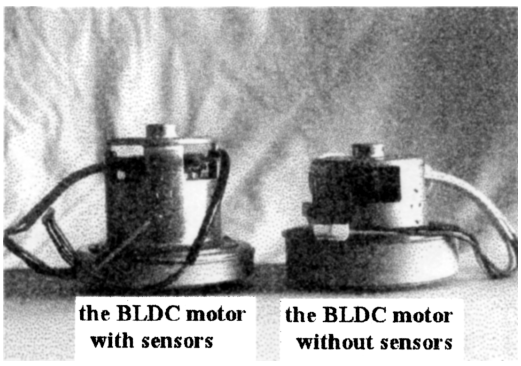

Fig. 14. The brushless DC motors with and without sensors.

signed for the high rotation speed. Figure 11 shows the waveforms of the terminal voltage V_{phv} and the phase current I_{phv} at 21,000 rpm, and Fig. 12 shows the phase current waveform at 5100 rpm. From Figs. 11 and 12, it is seen that the proposed method can be applied to high-speed rotation and is usable over a wide rotation range. More detailed examination of the speed controllable range will be conducted in the future. However, the BLDC motor performed entirely without stepping out under these experiments, showing that the starting sequence is very effective and stable.

Finally, Fig. 13 shows an experimental result that compares the proposed method with the control method using Hall sensors [23]. From Fig. 13, the phase current waveform (thin line) using the control method [23] is sharper and of larger amplitude. Moreover, the rise time t_1 is about 1.9 times as long as the fall time t_2. Then, the excitation timing collapses and the motor efficiency falls, while at the same time the magnetic noise and the rotational unevenness are increased. A possible cause may be error in determining the sensor position. On the other hand, the result of the proposed method has 20% smaller amplitude than the control method [23]. Thus, the BLDC motor using the proposed method can be rotated smoothly and quietly with high efficiency. But the proposed method may return the rotor at a smaller angle to the predetermined reset position in the position reset mode, making it difficult to apply to position control servomotors. However, the proposed method can be satisfactorily applied to drive motors such as pump motors, fan motors, and so on.

6. Conclusions

In this paper, a new sensorless drive system for a BLDC motor using position sensorless detection and PWM current control has been proposed. The stability of the DPLL open loop was verified, and a method of extracting correct phase information from the BEMF using the DPLL was shown. Next, a new starting sequence appropriate to the dynamic characteristics of the BLDC motor was proposed. Assured, stable starting movement of the BLDC motor was realized. The driver cost of the proposed method was 33% lower than that of the control method [23], and the motor cost was reduced by 15% compared with a BLDC motor with Hall sensors. Moreover, from these experimental results, it is seen that the proposed method can be used for high-speed rotation and over a wide rotation range.

Furthermore, even if the motor load has a certain amount of change, the BLDC motor can be rotated without stepping out, and speed control can be performed correctly.

Acknowledgment

This research was funded in part by an Intensive Development Research Promotion Enterprise Subsidy of the Fukushima Technology Center 1998, for which we express our gratitude.

REFERENCES

1. Ben-Brahim L. Motor speed identification via neural networks. IEEE/IAS Magazine, Jan./Feb., p 28–32, 1995.
2. Chaimers BJ et al. Variable-frequency synchronous motor drive for electric vehicles. IEEE Trans Ind Appl 1996;32:896–903.
3. Li Y, Walls TA, Loyd JD, Skinner JL. A novel two-phase BPM drive system with high power density and low cost. IEEE Trans Ind Appl 1998;34:1072–1080.
4. Williamson S, Boger MS. Impact of inter-bar currents on the performance of the brushless doubly fed motor. IEEE Trans Ind Appl 1999;35:435–460.
5. Marushima K et al. Speed control of the brushless DC motor contained magnetic abnormal-conditions type differential resolver. Trans IEE Japan 1998;118-D:1352–1360.
6. Ogasawara S et al. Method of controlling a permanent magnet synchronization eggplant motor. IEE Japan Proc, S.9-3, 1998.
7. Mizutani R, Takeshita T, Matsui N. Current model-based sensorless drivers of salient-pole PMSM at low speed and standstill. IEEE Trans Ind Appl 1998;34:841–846.
8. Takeshita T et al. Initial position angle selection for a sensorless brushless DC motor. Trans IEE Japan 1996;116-D:736-742.
9. Tomita T. Position and speed sensorless control of a cylinder type brushless DC motor for speed adaptation identification with a disturbance observer. Trans IEE Japan 1997;117-D:1205–1211.
10. Chen Z et al. Position sensorless control of a brushless DC motor by adaptation observer. Trans IEE Japan 1998;118-D:828–835.
11. Yang G et al. Position sensorless control of a brushless DC motor by adaptation observer. Trans IEE Japan 1993;113-D:579–586.
12. Tomita T et al. Position and speed sensorless control for a brushless DC motor by an adaptation slide observer. Trans IEE Japan 1995;115-D:765–774.
13. Hanamoto T et al. Sensorless control of BLDCM using extended BEMF observer. Trans IEE Japan 1998;118-D:1089–1090.
14. Bolognani S, Oboe R, Zigliotto M. Sensorless full-digital PMSM drive with EKF estimation of speed

and rotor position. IEEE Trans Ind Electron 1999;46:184–191.
15. Tatematsu K et al. New approaches with sensorless drives. IEEE Ind Appl Mag 2000;6:44–50.
16. Takeshita T et al. Control of the sensorless permanent magnet type synchronous electric motor at the time of electric resupply. Trans IEE Japan 1998;118-D:1443–1449.
17. Kasa T et al. A method of rectifying the estimation error of a sensorless brushless DC motor by neuro-fuzzy technology. Trans IEE Japan 1998;118-D:186–192.
18. Ohta K et al. Drive stability at the time of direct-current power supply voltage change of a sensorless brushless DC motor. 1998 Institute of Electrical Engineers of Japan Industrial Application Section National Conference, p 59–62.
19. Xu BH, Tsuji T et al. Construction of position sensorless control of a BLDC motor. 1999 Institute of Electrical Engineers of Japan, Industrial Application Section, National Conference, 5-30/31, 1999.
20. Endo Z. Sensorless control of a trapezoid drive motor. '93 Motor Technical Symposium, B4-2-1/8.
21. Nagatake K. Motor inverter technology for household electric appliances. Nikkan Kogyo Shimbun; 2000. p 86–94.
22. Kenjyo T et al. New brushless motors. Sogo Electronic Publishing Company; 2000. p 79–87.
23. Iijima M. Speed control device of a brushless motor. Patent 2679879th, Patent official report S9-2679879.
24. Ozawa R. PLL frequency synthesizer and circuitry method. Sogo Electronic Publishing Company; 1994.
25. Stensby JL. Phase-locked loops. CRC Press; 1997.
26. Dote Y et al. Fundamentals of brushless servo motors, and their applications. Sogo Electronic Publishing Company; 1985. p 199–204.
27. Hanselman DC. Brushless permanent-magnet motor design. McGraw–Hill; 1994.
28. Adachi S. Control engineering. Tokyo Denki University Publications Office; 1999.
29. Xu BH et al. Sensorless drive of a brushless DC motor using a digital phase synchronous loop. Japanese Patent Application No. 11-235524, 1999.
30. Borse GJ. Numerical methods with MATLAB. PWS Publishing Company; 1997.

AUTHORS (from left to right)

Yoko Amano (formerly Bing Hong Xu) (member) received his B.S. degree from the East Normal University of China in 1983, M.S. degree from Shanghai University in 1988, and D.Eng. degree from the University, Japan in 1997, all in system engineering. He is currently a vice-chief in the technical management department of Yamamoto Electric Corporation. From 1983 to 1990, he was a lecturer in the Electrical Engineering Department of Shanghai Building Materials Industrial Institute. From 1990 to 1991, he was a visiting scholar at Oida University. His research interests include intelligent control of complex systems, control systems, power electronics, and motion control. He is a member of the IEEE Industry Applications Society and the Institute of Electrical Engineers of Japan.

Toshio Tsuji (member) received his B.E. degree in industrial engineering in 1982, and M.E. and D.Eng. degrees in system engineering in 1985 and 1989, all from Hiroshima University. From 1985 to 1994, he was a research associate at Hiroshima University, and a visiting researcher at the University of Genoa, Italy, from 1992 to 1993. He is currently a professor of artificial complex systems engineering at Hiroshima University. He has been interested in various aspects of motor control in robot and human movements. His current interests focus on distributed planning and learning of motor coordination.

AUTHORS (continued) (from left to right)




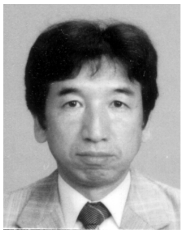

Atsushi Takahashi (member) received his M.S. degree in electronic engineering from Akita University in 1983 and became a researcher at Fukushima Technology Center. His research interests include image processing, EMI suppression, multiprocessor designs, and motor control system designs using DSP and FPGA. He is a member of IEICE and the Institute of Electrical Engineers of Japan.

Shigeo Ouchi (nonmember) received his B.S. degree from the Faculty of Engineering of Yamagata University in 1988. He designed measuring instruments at Anritsu Corporation from 1988 to 1994. He became a researcher at Fukushima Technology Center in 1994. His research interests include image processing, EMI suppression, multiple processor designs, and motor control system designs using DSP and FPGA.

Kyoji Hamatsu (nonmember) received his B.S. degree in electronic engineering from Nihon University in 1975 and joined Yamamoto Electric Corporation. He is currently a manager in the Technical Management Department. His research interests include control systems, power electronics, motion control, motor drivers, and magnetic field analysis.

Masahiko Iijima (member) received his B.S. degree in applied physics from Tokai University in 1978. He joined Yamamoto Electric Corporation in 1985 and is currently chief of the Management Department. His research interests are motor control circuits and software development. He is a member of the Institute of Electrical Engineers of Japan.